RAPID COMMUNICATIONS

PHYSICAL REVIEW B VOLUME 47, NUMBER 22 1 JUNE 1993-II

Rapid Communications

Rapid Communications are intended for the accelerated publication of important new results and are therefore given priority treatment both in the editorial office and in production. A Rapid Communication in **Physical Review B** *should be no longer than four printed pages and must be accompanied by an abstract. Page proofs are sent to authors.*

Burgers vector of dislocations in an icosahedral $Al_{62}Cu_{25.5}Fe_{12.5}$ quasicrystal determined by means of convergent-beam electron diffraction

R. Wang and M. X. Dai

Department of Physics, Wuhan University, 430072 Wuhan, China

and Beijing Laboratory of Electron Microscopy, Chinese Academy of Sciences, P.O. Box 2724, 100080 Beijing, China

(Received 25 February 1993)

Dislocations in an $Al_{62}Cu_{25.5}Fe_{12.5}$ face-centered icosahedral quasicrystal were studied by means of the contrast experiment and defocus convergent-beam electron diffraction technique. The indices of the six-dimensional Burgers vector of the dislocations were determined to be $\frac{1}{2}[1\,-1\,1\,-1\,0\,0]$. The projection $\mathbf{b}_{\parallel}$ of this six-dimensional Burgers vector in the three-dimensional physical space is exactly parallel to a twofold axis of the icosahedron. The magnitude $|\mathbf{b}_{\parallel}|=0.291$ nm was calculated when $a=0.896$ nm is taken for the lattice constant of the face-centered icosahedral phase.

Tanaka, Ueno, and Harada[1] developed a defocus convergent-beam electron diffraction (CBED) technique to obtain large-angle CBED patterns. In the defocus CBED technique the crossover of the convergent incident beam does not lie exactly on the foil specimen for transmission electron microscopy (TEM), as in the conventional CBED technique, but instead lies below (see Fig. 1) or above the specimen plane. There is a shadow image of the illuminated specimen region superimposed on the defocus CBED pattern. For example, Fig. 1 shows that the dislocation *DD* in the illuminated specimen region forms shadow images *D'D'* on the (000)-transmitted and (*hkl*)-diffracted disks. Therefore a large strain-field region of a defect can be studied simultaneously by the defocus CBED technique, and hence this technique has extensively been used to determine the geometric parameters of defects in crystals, e.g., the Burgers vector **b** of a dislocation (see the next paragraph).

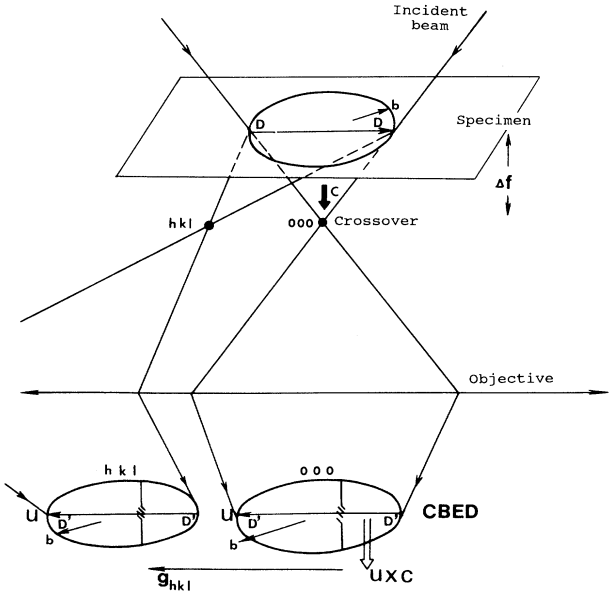

FIG. 1. Ray diagram of the defocus CBED technique and the splitting of shifting behavior of the higher-order $\mathbf{g}_{hkl}$ reflection fringe induced by the dislocation *DD* with the Burgers vector **b**.

Carpenter and Spence[2] found that a dislocation illuminated by the convergent incident beam induces the higher-order reflection fringes to be split when $\mathbf{g}\cdot\mathbf{b}\neq 0$ with **g** being the reciprocal vector of the reflection fringe, and has no splitting effect when $\mathbf{g}\cdot\mathbf{b}=0$. Thus one can determine the direction of the Burgers vector **b** of a dislocation by finding two unsplit reflection fringes. Cherns and Preston[3] pointed out that in a defocus CBED pattern, the higher-order reflection fringes split into $n+1$ lines with n nodes ($\mathbf{g}\cdot\mathbf{b}=n$). For example, in the schematic diagram shown in Fig. 1 the **g** fringe splits into three nodes because in this case $\mathbf{g}\cdot\mathbf{b}=3$. By using the Cherns-Preston rule, one can determine the magnitude of the Burgers vector. Recently, Wen, Wang, and Lu[4] and Niu, Wang, and Lu[5] proposed a criterion for the shift direction of the fringes. They introduced a vector **c** pointed to the crossover of the incident beam from the illuminated specimen and proposed that on the $\mathbf{u}\times\mathbf{c}$ side of the shadow image of a dislocation with a line direction **u** and the Burgers vector **b**, the split higher-order reflection fringe shifts along the **b** direction. This criterion is shown in Fig. 1 schematically. Combining the Cherns-Preston rule and this criterion, it is possible to determine the Burgers vector **b**, including its direction, magnitude, and sign (sense), of a dislocation in crystals by means of the defocus CBED technique.[5,6]

Since the discovery of quasicrystals (QC's),[7] many authors studied defects, especially dislocations, in QC's. For example, Hiraga and Hirabayashi[8] observed disloca-

tions in the Al-Mn-Si icosahedral quasicrystal (IQC) by high-resolution electron microscopy (HREM). Under the supposition that edge dislocations in IQC's occur on the planes perpendicular to the symmetry axes and the dislocation lines along one of the symmetry axes in the plane, Wang *et al.*[9] determined the Burgers vectors $\mathbf{b}_\parallel$ of edge dislocations in IQC by means of HREM and image processing. Devaud-Rzepski, Cornier-Quiquandon, and Gratias[10] determined the Burgers vector by means of HREM and under the supposition of minimum length of $\mathbf{b}_\parallel$. Zhang, Wollgarten, and Urban[11] determined the direction of the Burgers vector $\mathbf{b}_\parallel$ of dislocations in the $Al_{65}Cu_{20}Fe_{15}$ IQC to be parallel to a twofold axis of the icosahedron. Dai[12] estimated the magnitude of the Burgers vector $\mathbf{b}_\parallel$ of a dislocation in $Al_{62}Cu_{25.5}Fe_{12.5}$ IQC from only the parallel space. However, until now, there has been no work determining the indices of a six-dimensional (6D) Burgers vector $\tilde{\mathbf{b}}$ of dislocations in IQC's without any presuppositions.

Wang and Cheng[13] applied the dynamical theory of electron diffraction of crystals to the case of IQC's containing defects. They pointed out that both the existing wave-optical and wave-mechanical representations of the dynamical theory of electron diffraction can also be applied to the QC case except that the phase term $\mathbf{g}\cdot\mathbf{R}$ in these expressions must be replaced by a 6D inner product $\tilde{\mathbf{g}}\cdot\tilde{\mathbf{R}}$, where $\tilde{\mathbf{g}}$ and $\tilde{\mathbf{R}}$ are the 6D reciprocal vector and displacement vector, respectively. Therefore the Cherns-Preston rule[3] and the criterion proposed by Wen, Wang, and Lu[4] and Niu, Wang, and Lu[5] can be applied to dislocations in QC's by changing the term $\mathbf{g}\cdot\mathbf{b}$ into $\tilde{\mathbf{g}}\cdot\tilde{\mathbf{b}}$.

In the present paper we report the results of a complete determination of the 6D Burgers vector $\tilde{\mathbf{b}}$ of dislocations in the $Al_{62}Cu_{25.5}Fe_{12.5}$ face-centered IQC by means of the defocus CBED technique.

Figure 2 is a stereographic projection of IQC showing the directions of the 3D projections $\mathbf{e}_\parallel^i$ $(i=1,2,\ldots,6)$ of the 6D basis vectors. The indices of the 6D reciprocal vector $\tilde{\mathbf{g}}$ and 6D burgers vector $\tilde{\mathbf{b}}$ used in the present work are all related to these basis vectors.

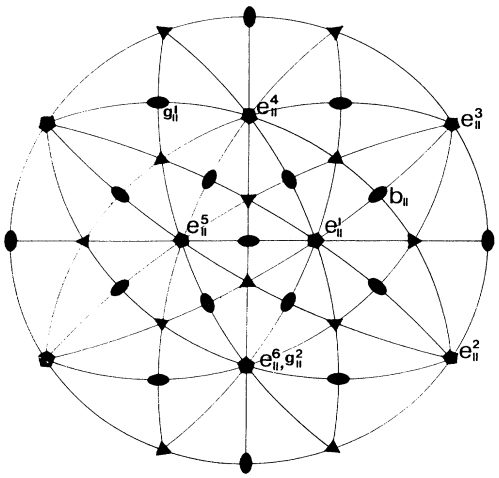

FIG. 2. Stereographic projection of the IQC. $\mathbf{e}_\parallel^i$ $(i=1,2,\ldots,6)$ are the projections in 3D physical space of the 6D basis vectors. $\mathbf{b}_\parallel$ designates the direction of the projection of the 6D Burgers vector $\mathbf{b}$ in the 3D physical space.

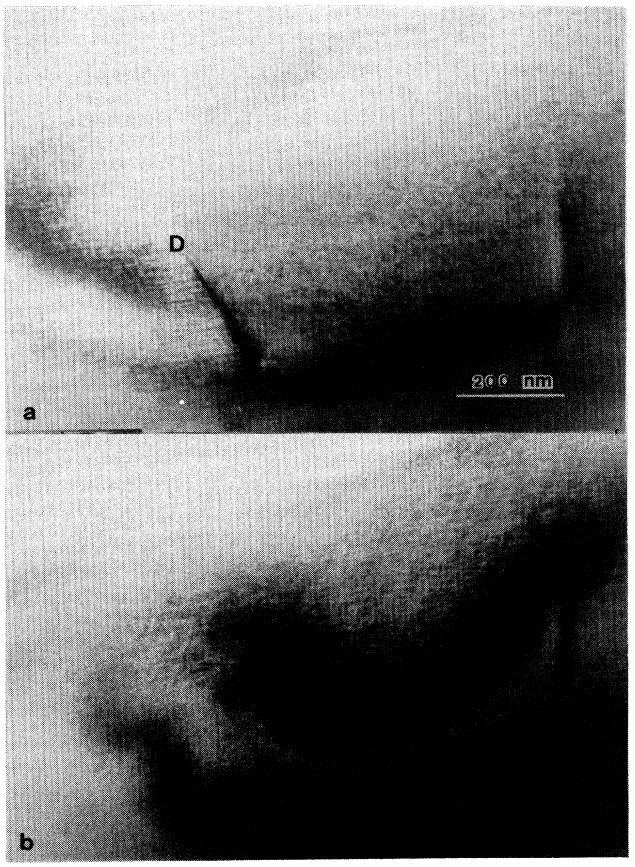

FIG. 3. Bright-field images under approximate two-beam conditions of the studied dislocation *DD* in the $Al_{62}Cu_{25.5}Fe_{12.5}$ IQC. (a) $\tilde{\mathbf{g}}_0=(0\,4\,-4\,-6\,0\,6)$, in contrast. (b) $\tilde{\mathbf{g}}_1=(0\,-4\,0\,4\,2\,-2)$, out of contrast.

Under the $\tilde{\mathbf{g}}_0=(0\,4\,-4\,-6\,0\,6)$ two-beam condition, we observed the bright-field (BF) image of a dislocation *DD* shown in Fig. 3(a). When reflection $\tilde{\mathbf{g}}_1=(0\,-4\,0\,4\,2\,-2)$ or $\tilde{\mathbf{g}}_2=(2\,2\,-2\,-2\,2\,4)$ is excited, the contrast of the dislocation *DD* vanishes, as shown in Fig. 3(b), which means $\tilde{\mathbf{g}}_1\cdot\tilde{\mathbf{b}}=0$ and $\tilde{\mathbf{g}}_2\cdot\tilde{\mathbf{b}}=0$. As will be discussed at the end of this paper, the perpendicular components of these strong reflections are rather small, and hence $\mathbf{g}_\perp^1\cdot\mathbf{b}_\perp\cong 0$ and $\mathbf{g}_\perp^2\cdot\mathbf{b}_\perp\cong 0$. Therefore we have

$$\mathbf{g}_\parallel^1\cdot\mathbf{b}_\parallel\cong 0,\quad \mathbf{g}_\parallel^2\cdot\mathbf{b}_\parallel\cong 0\ , \tag{1}$$

from which it is easy to determine the direction of the $\mathbf{b}_\parallel$ vector which is nearly parallel to a twofold axis designated in Fig. 2 together with the directions $\mathbf{g}_\parallel^1$ and $\mathbf{g}_\parallel^2$.

In order to determine the 6D Burgers vector $\tilde{\mathbf{b}}$ of this dislocation uniquely we carried out a defocus CBED experiment. Figure 4 shows such a pattern when the dislocation *DD* is illuminated by a convergent incident beam with a defocus $\Delta f=3$ μm. Three reflection fringes, $\tilde{\mathbf{g}}_3$, $\tilde{\mathbf{g}}_4$, and $\tilde{\mathbf{g}}_5$, across the shadow image *D'D'* of the dislocation split, respectively, into $n_3=2$, $n_4=2$, and $n_5=1$

nodes. The diffracted disks and the corresponding reciprocal vectors $\mathbf{g}_{\|}^{3}$, $\mathbf{g}_{\|}^{4}$, and $\mathbf{g}_{\|}^{5}$ are also shown in Fig. 4. According to the Chern-Preston rule, we conclude that

$$\tilde{\mathbf{g}}_3\cdot\tilde{\mathbf{b}}=\pm 2,\quad \tilde{\mathbf{g}}_4\cdot\tilde{\mathbf{b}}=\pm 2,\quad \tilde{\mathbf{g}}_5\cdot\tilde{\mathbf{b}}=\pm 1\ . \tag{2}$$

On the $\mathbf{u}\times\mathbf{c}$ side of the shadow image $D'D'$ of the dislocation, these fringes shift to the left-hand side. Hence we can deduce the approximate direction of $\mathbf{b}_{\|}$, as shown in Fig. 4, according to the criterion proposed by Wen *et al.*[4] Noticing the directions of the $\mathbf{g}_{\|}^{3}$, $\mathbf{g}_{\|}^{4}$, and $\mathbf{g}_{\|}^{5}$ reciprocal vectors, as shown in Fig. 4, the signs of the numbers ± 2, ± 2, and ± 1 in Eq. (2) can be deduced to be

$$\tilde{\mathbf{g}}_3\cdot\tilde{\mathbf{b}}=-2,\quad \tilde{\mathbf{g}}_4\cdot\tilde{\mathbf{b}}=-2,\quad \tilde{\mathbf{g}}_5\cdot\tilde{\mathbf{b}}=+1\ . \tag{3}$$

We observed in the present work 13 reflection fringes in six defocus CBED patterns. From their splitting and shifting behaviors, we obtain 13 equations similar to Eq. (3). Together with Eq. (1), there are 15 such equations.

In order to determine the indices of $\tilde{\mathbf{b}}=[b_1b_2b_3b_4b_5b_6]$, it is necessary to index the reflections $\tilde{\mathbf{g}}_1,\tilde{\mathbf{g}}_2,\ldots,\tilde{\mathbf{g}}_{15}$. Based on Elser's work,[14] Dai and Wang[15] proposed a method to calculate the geometric distribution of reflection fringes in CBED patterns. By this method, we indexed these reflections (except $\tilde{\mathbf{g}}_5$), as listed in Table I, together with the splitting nodes n_i of the reflection fringes and other related quantities. $\tilde{\mathbf{g}}_5$ possesses less intensity and was indexed to be $\tilde{\mathbf{g}}_5=(-1\,5\,-5\,-9\,9\,3)$ from the consideration of the geometric distribution of this reflection fringe. Thus we obtain the following linear equation set expressed in matrix form:

$$\mathbf{A}\mathbf{b}^t=n^t\ , \tag{4}$$

with $\mathbf{A}$ being a 15×6 matrix consisting of the indices $h_1,h_2,\ldots,h_6$ of the 15 reflections $\tilde{\mathbf{g}}_i$ and $\mathbf{n}^t$ being a 15×1 matrix consisting of the splitting nodes n_i, as listed in Table I. Here and afterward, t designates transpose of a matrix.

If the rank of the matrix $\mathbf{A}$ were less than 6, then we could not obtain a unique solution for the indices b_i of $\tilde{\mathbf{b}}$,

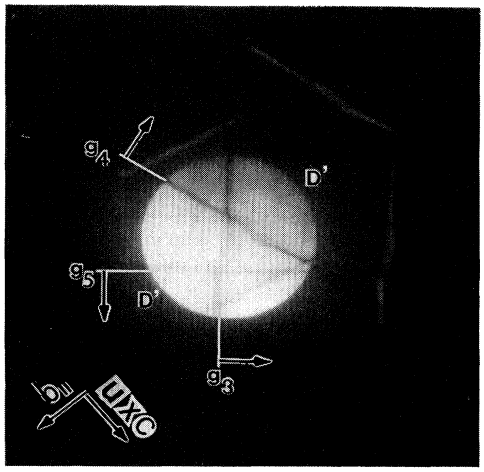

FIG. 4. Defocus CBED pattern when the incident beam illuminates the dislocation DD with shadow images $D'D'$.

and more reflections would be needed. Simple calculation shows that the rank of the matrix $\mathbf{A}$ is 6 and Eq. (4) may be simplified to

$$\mathbf{c}\mathbf{b}^t=\mathbf{m}^t\ , \tag{5}$$

with

$$\mathbf{c}=\begin{bmatrix} 0 & -4 & 0 & 4 & 2 & -2 \\ 2 & 2 & -2 & -2 & 2 & 4 \\ 4 & 8 & 6 & -2 & -4 & 2 \\ 2 & 2 & 8 & 4 & -4 & -6 \\ -4 & -10 & -2 & 6 & 4 & -4 \\ 4 & -2 & 6 & 8 & 2 & -4 \end{bmatrix}$$

and

$$\mathbf{m}=[0\,0\,2\,2\,-1\,2]\ .$$

By solving the linear equation set (5) we obtain the following indices of the 6D Burgers vector $\tilde{\mathbf{b}}$:

TABLE I. Six-dimensional indices h_i, splitting nodes n_i, and related quantities of the studied reflections $\tilde{\mathbf{g}}_i$. The magnitudes $|\tilde{g}|$, $|g_{\|}|$, and $|g_{\perp}|$ are in nm^{-1}. $\tilde{\mathbf{b}}=\frac{1}{2}[1\,-1\,1\,-1\,0\,0]$, $|b_{\|}|=0.291$ nm, $|b_{\perp}|=1.234$ nm.

$\tilde{\mathbf{g}}_i$	h_1	h_2	h_3	h_4	h_5	h_6	n_i	$\mathbf{g}_{\|}\cdot\mathbf{b}_{\|}$	$\mathbf{g}_{\perp}\cdot\mathbf{b}_{\perp}$	$\lvert\tilde{g}\rvert$	$\lvert g_{\|}\rvert$	$\lvert g_{\perp}\rvert$
$\tilde{\mathbf{g}}_1$	0	−4	0	4	2	−2	0	0	0	4.99	4.97	0.45
$\tilde{\mathbf{g}}_2$	2	2	−2	−2	2	4	0	0	0	4.74	4.73	0.26
$\tilde{\mathbf{g}}_3$	4	8	6	−2	−4	2	2	1.90	0.11	9.34	9.33	0.38
$\tilde{\mathbf{g}}_4$	2	2	8	4	−4	−6	2	1.90	0.11	9.34	9.33	0.38
$\tilde{\mathbf{g}}_5$	−1	5	−5	−9	9	3	−1	−1.17	0.17	11.76	9.34	7.14
$\tilde{\mathbf{g}}_6$	2	8	−2	−8	−2	8	0	0	0	11.27	11.27	0.15
$\tilde{\mathbf{g}}_7$	0	−6	0	6	4	−4	0	0	0	8.05	8.04	0.28
$\tilde{\mathbf{g}}_8$	−4	−10	−2	6	4	−6	−1	−1.17	0.17	11.38	11.38	0.39
$\tilde{\mathbf{g}}_9$	4	−2	6	8	2	−4	2	1.89	0.11	9.34	9.33	0.38
$\tilde{\mathbf{g}}_{10}$	6	8	4	−2	−2	4	2	1.90	0.11	9.34	9.33	0.38
$\tilde{\mathbf{g}}_{11}$	−8	−8	−2	2	−2	−8	−2	−1.90	−0.11	11.27	11.27	0.15
$\tilde{\mathbf{g}}_{12}$	2	−2	8	8	−2	−8	2	1.90	0.11	11.27	11.27	0.15
$\tilde{\mathbf{g}}_{13}$	−8	−8	−8	−2	2	−2	−3	−3.07	0.07	−11.27	11.27	0.15
$\tilde{\mathbf{g}}_{14}$	−8	−2	−8	−8	−2	2	−3	−3.06	0.07	−11.27	11.27	0.15
$\tilde{\mathbf{g}}_{15}$	−10	−6	−10	−6	0	0	−4	−3.79	−0.21	−13.02	13.02	0.17

$\tilde{\mathbf{b}}=\frac{1}{2}[1\,-1\,1\,-1\,0\,0]$.

From this expression, it is easy to calculate the projections of the 6D Burgers vector $\tilde{\mathbf{b}}$ in the 3D physical space ($\mathbf{b}_\parallel$) and in the 3D pseudo (perpendicular) space ($\mathbf{b}_\perp$). The direction of $\mathbf{b}_\parallel$ is shown in Fig. 2 and is exactly parallel to a twofold axis as determined by the contrast experiment. Its magnitude is $|\mathbf{b}_\parallel|=0.291$ nm when the value $a=0.896$ nm is chosen for the lattice constant of the face-centered icosahedral $Al_{62}Cu_{25.5}Fe_{12.5}$ phase as measured and discussed by Dai and Wang[16] and references cited therein. Similarly, we calculated the magnitude $|b_\perp|=1.23$ nm and the ratio $|b_\perp|/|b_\parallel|=4.23$, which is less than that proposed by Wollgarten, Zhang, and Urban.[17,18]

Similarly, we calculated the projections $\mathbf{g}_\parallel$ and $\mathbf{g}_\perp$ of the 6D reciprocal vectors $\tilde{\mathbf{g}}$ in the physical and pseudo spaces and then the values of $\mathbf{g}_\parallel\cdot\mathbf{b}_\parallel$ and $\mathbf{g}_\perp\cdot\mathbf{b}_\perp$, which are listed in Table I. From Table I, it is clear that the magnitudes $|g_\perp|$ for all strong reflections are rather small (<0.45 nm^{-1}), and hence all the ratios $\mathbf{g}_\perp\cdot\mathbf{b}_\perp/\mathbf{g}_\parallel\cdot\mathbf{b}_\parallel$ are small (<0.15), except the case when $\mathbf{g}_\parallel\cdot\mathbf{b}_\parallel=\mathbf{q}_\perp\cdot\mathbf{b}_\perp=0$. This is a general situation for the contrast experiment and the CBED experiment, which concerns higher-order reflections. In the contrast experiment one excites usually strong reflections that have small $|g_\perp|$ values according to Elser[14] and our own calculation.[19] The intensities of the concerned higher-order reflections in the CBED experiment are weaker than those for the contrast experiment but still stronger than other higher-order reflections. These concerned higher-order reflections have small $|g_\perp|$ values as well. Their lower intensities compared to the lower-order reflections have the origin that the atomic scattering factor decreases with the increase of the magnitude of $|g_\perp|$. Moreover, when we treat the experimental data listed in Table I of Dai's paper[12] by the method proposed in this paper, we obtain the 6D Burgers vector $\tilde{\mathbf{b}}=\frac{1}{2}[0\,-1\,1\,0\,-1\,1]$.

In summary, we have determined the 6D Burgers vector of dislocations in $Al_{62}Cu_{25.5}Fe_{12.5}$ IQC by means of defocus CBED. This is a complete experimental method that can be applied to any type of dislocations in QC's without any presupposition about the Burgers vector. This method may become a standard technique to determine Burgers vectors in QC's.

This project was supported in part by the National Natural Science Foundation of China. One of the authors (M.X.D.) would like to thank Professor K. Urban, Forschungszentrum, Jülich, Germany, where some preliminary experimental work was carried out.

[1]M. Tanaka, K. Ueno, and Y. Harada, J. Electron Microsc. **29**, 408 (1980).
[2]R. W. Carpenter and J. C. H. Spence, Acta Crystallogr. Soc. A **38**, 55 (1982).
[3]D. Cherns and A. R. Preston, J. Electron Microsc. Suppl. **35**, 721 (1986).
[4]J. Wen, R. Wang, and G. Lu, Acta Crystallogr. Sec. A **45**, 422 (1989).
[5]F. Niu, R. Wang, and G. Lu, Acta Crystallogr. Sec. A **47**, 36 (1991).
[6]M. Tanaka, M. Terauchi, and T. Kaneyama, J. Electron Microsc. **40**, 211 (1991).
[7]D. Shechtman, I. Blech, D. Gratias, and J. W. Cahn, Phys. Rev. Lett. **53**, 1951 (1984).
[8]K. Hiraga and M. Hirabayashi, Jpn. J. Appl. Phys. **26**, L155 (1987).
[9]D. N. Wang, T. Ishimasa, H. U. Nissen, S. Hovmoller, and J. Rhyner, Philos. Mag. **A58**, 737 (1988).
[10]J. Devaud-Rzepski, M. Cornier-Quiquandon, and D. Gratias, in *Proceedings of the Third International Conference on Quasicrystals,* edited by M. J. Yacaman, D. Romeu, V. Castano, and A. Gomez (World Scientific, Singapore, 1989), p. 498.
[11]Z. Zhang, M. Wollgarten, and K. Urban, Philos. Mag. Lett. **61**, 125 (1990).
[12]M. X. Dai, Philos. Mag. Lett. **66**, 235 (1992).
[13]R. Wang and Y. Cheng, Mater. Sci. Forum **22-24**, 409 (1987).
[14]V. Elser, Acta Crystallogr. Sec. A **42**, 36 (1986).
[15]M. Dai and R. Wang, Solid State Commun. **73**, 77 (1990).
[16]M. Dai and R. Wang, Acta Crystallogr. Sec. B **46**, 455 (1990).
[17]M. Wollgarten, Z. Zhang, and K. Urban, Philos. Mag. Lett. **65**, 1 (1992).
[18]M. Wollgarten, D. Gratias, Z. Zhang, and K. Urban, Philos. Mag. Lett. **A64**, 819 (1991).
[19]J. Feng, M. X. Dai, R. Wang, and H. Zou, J. Phys. Condens. Matter **4**, 9247 (1992).

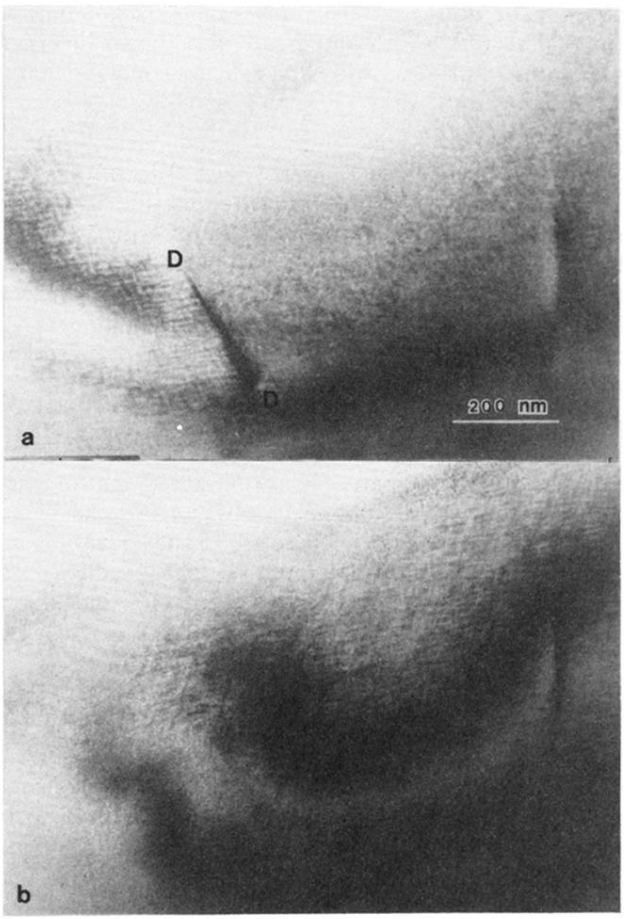

FIG. 3. Bright-field images under approximate two-beam conditions of the studied dislocation *DD* in the $Al_{62}Cu_{25.5}Fe_{12.5}$ IQC. (a) $\vec{g}_0=(0\,4\,\bar{4}\,\bar{6}\,0\,6)$, in contrast. (b) $\vec{g}_1=(0\,\bar{4}\,0\,4\,2\,\bar{2})$, out of contrast.

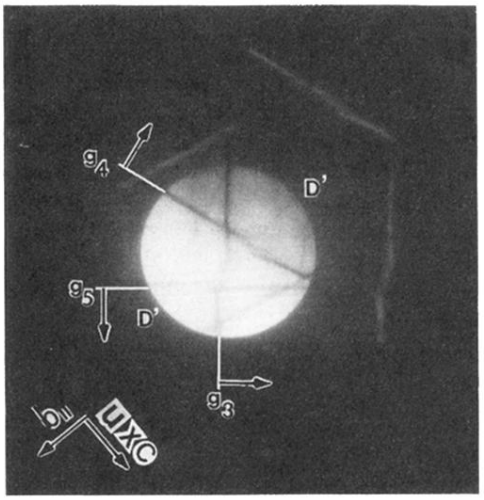

FIG. 4. Defocus CBED pattern when the incident beam illuminates the dislocation DD with shadow images $D'D'$.